Research Article

Maryana Handula, Dylan Chapeau, Yann Seimbille*

Orthogonal synthesis of a versatile building block for dual functionalization of targeting vectors

https://doi.org/10.1515/chem-2022-0361
received May 17, 2023; accepted June 28, 2023

Abstract: Dual functionalization of targeting vectors, such as peptides and antibodies, is still synthetically challenging despite the increasing demand for such molecules serving multiple purposes (i.e., optical and nuclear imaging). Our strategy was to synthesize a versatile building block via the orthogonal incorporation of chemical entities (e.g., radionuclide chelator, fluorescent dye, cytotoxic drugs, click handle, and albumin binder) in order to prepare various dual functionalized biovectors. The functional groups were introduced on the building block using straightforward chemical reactions. Thus, an azidolysine and a biogenic lysine were installed into the building block to allow the coupling of the second functional group and the regioselective conjugation to the biovector via the strain-promoted azide–alkyne cycloaddition, while the first functional group was inserted during the solid-phase peptide synthesis. To extend the applicability of the building block to large biomolecules, such as antibodies, a DBCO-maleimide linker was clicked to the azidolysine to present a maleimide group that could react with the exposed sulfhydryl groups of the cysteine residues. To exemplify the possibilities offered by the building block, we synthesized two dual-functionalized compounds containing a 2,2′,2″′,2″′-(1,4,7,10-tetraazacyclododecane-1,4,7,10-tetrayl) tetraacetic acid chelator and an albumin binder (**4a**) to extend the blood half-life of radiolabeled biovectors or a click handle (**4b**) to enable the late-stage click reaction; **4a** and **4b** were conjugated to a model cyclic peptide bearing a short thiolated linker at the *N*-terminal position, in a single step via the thiol–maleimide Michael addition. Both dual-functionalized peptides, **9a** and **9b**, were obtained rapidly in high chemical purity (>95%) and labeled with [^{111}In]$InCl_3$. Both radiopeptides showed good stability in mouse serum and PBS buffer.

Keywords: orthogonal reaction, SPAAC, thiol–maleimide Michael addition, biovector

1 Introduction

In the past decade, peptides and antibodies have gained a lot of attention for targeted imaging and therapy of different types of cancers [1–3]. The low molecular weight of peptides confers multiple advantages compared to larger biomolecules, such as antibodies. For instance, peptides are cleared faster from the blood circulation, they present faster pharmacokinetics (PK), and they have better penetration into the malignant tissue [4]. However, antibodies are known to exhibit a remarkable binding selectivity and affinity to the targeted antigens. Therefore, peptides and antibodies are getting more and more used for a panoply of applications for which chemical modifications of these biomolecules are required. Several functional groups have been recently considered to modify these biovectors, such as imaging probes (i.e., radiometal chelator and fluorescent dye) for non-invasive molecular imaging and fluorescence-guided surgery, cytotoxic drugs for small molecule- or antibody-drug conjugates, PK modifiers (i.e., albumin binder and cleavable linker) to improve their PK. The trend was initially to develop a mono-functionalized compound for each application. However, due to the rise of combined applications (i.e., multimodality imaging, targeted therapy, and companion diagnostic) and cost-effectiveness, the dual functionalization of biomolecules is getting more and more popular.

The introduction of these functional groups into these biomolecules was usually achieved via the amidation of lysine residues present in the peptide or protein sequence [5,6]. However, this approach is either synthetically challenging or lacks regioselectivity. For peptide vectors, it is possible to select appropriate protecting groups during the solid-phase peptide synthesis (SPPS) to thwart these limitations. However, few functional groups, such as fluorescent cyanine dyes or *trans*-cyclooctene (TCO) click handles, are

*** Corresponding author: Yann Seimbille**, Department of Radiology and Nuclear Medicine, Erasmus MC Cancer Institute, Erasmus University Medical Center Rotterdam, Rotterdam, 3015 GD, The Netherlands; Life Sciences Division, TRIUMF, Vancouver, BC V6T 2A3, Canada, e-mail: y.seimbille@erasmusmc.nl, tel: +31-10-703-8961
Maryana Handula, Dylan Chapeau: Department of Radiology and Nuclear Medicine, Erasmus MC Cancer Institute, Erasmus University Medical Center Rotterdam, Rotterdam, 3015 GD, The Netherlands

too sensitive to bear the harsh conditions occurring during the synthesis (e.g., acidic and basic conditions) [7,8]. Therefore, alternative synthetic routes are required to functionalize these biovectors under friendly conditions. We recently described the synthesis of a multifunctional single-attachment-point to prepare dual fluorescent/nuclear-labeled biovectors [9,10]. Herein, we report the applicability of a building block allowing the dual functionalization of biovectors. The synthetic approach was based on the chemoselective attachment of the functional groups using straightforward chemical reactions, such as the strain-promoted azide–alkyne cycloaddition (SPAAC), the thiol–maleimide Michael addition or the inverse electron-demand Diels Alder (IEDDA) reaction. These reactions are known to be orthogonal, to occur under biologically friendly conditions, and the end-product is stable [11].

As a proof-of-concept, we synthesized two building blocks, **4a** and **4b**, functionalized with a 2,2′,2″,2‴-(1,4,7,10-tetraazacyclododecane-1,4,7,10-tetrayl) tetraacetic acid (DOTA) chelator for complexation of imaging and therapeutic radionuclides (e.g., indium-111, gallium-68, lutetium-177, and actinium-225). Additionally, an azidolysine and a lysine were incorporated into the building block to provide two attachment points dedicated to the coupling of the second functional group and conjugation of the building block to the biovector. The side-chain of the lysine was used to attach an albumin-binding moiety (**4a**) or a TCO (**4b**), whereas a dibenzocyclooctyne (DBCO)–maleimide linker was clicked to the azide group. The linker was inserted to increase the distance between the building block and the biovector and to provide a maleimide group that could react selectively with the cysteine residues present in antibodies. To demonstrate the versatility of our dual-functionalized building block, **4a** and **4b** were conjugated to a model cyclic peptide. The final compounds, **9a** and **9b**, were radiolabeled with [^{111}In]$InCl_3$, and their stability in PBS buffer and mouse serum was investigated.

2 Materials and methods

2.1 General information

The chemicals and solvents were obtained from commercial suppliers and used without further purification unless specified. SPPS, based on the Fmoc strategy, was performed manually using manual reaction vessels (Chemglass, Vineland, United States). DOTA-NHS-ester was acquired from Macrocyclics (Plano, TX, USA) and [^{111}In]$InCl_3$ (370.0 MBq/mL in HCl, pH 1.5–1.9) was purchased from Curium (Petten, The Netherlands). High-performance liquid chromatography (HPLC) and mass spectrometry (MS) analyses were acquired on an Agilent 1260 Infinity II LC-MS system (Middelburg, The Netherlands). Instant thin-layer chromatography (iTLC) analysis was performed on plates of silica gel-impregnated glass fiber sheets. The plates were eluted with sodium citrate (0.1 M, pH 5). They were analyzed using a Brightspec bSCAN radio-chromatography scanner (Antwerp, Belgium) supplied with a sodium iodide detector. The radioactive samples were counted using a Perkin Elmer Wizard 2480 gamma counter (Waltham, MA, USA). Radioactivity determination was performed using the VDC-405 dose calibrator (Comecer, Joure, The Netherlands). Quality control of the compounds was carried out using an analytical column from Agilent (Poroshell 120, EC-C18, 2.7 µm, 3.0 × 100 mm) under a gradient elution of acetonitrile (ACN) from 5 to 100% in H_2O, containing 0.1% formic acid (FA) using a flow rate of 0.5 mL/min for 8 min. Purification of compounds **3**, **4a**, and **9a** was performed using a preparative Agilent 1290 Infinity II HPLC system and an Agilent 5 Prep C18 preparative column (50 × 21.2 mm, 5 µm) with a gradient elution of ACN (5–95% in H_2O containing 0.1% FA for 8 min) using a flow rate of 10 mL/min for 10 min. Purification of compounds **8**, **4b**, and **9b** was carried out using a semi-preparative Alliance HPLC system from Waters (Etten-Leur, The Netherlands). Purification of compound **8** was performed using a semi-preparative column (Phenomenex C-18 Luna®, 250.0 × 10.0 mm, 5 µm) with an isocratic elution of ACN (35% in H_2O containing 0.1% trifluoroacetic acid (TFA) using a flow rate of 3 mL/min for 30 min. Purification of compounds **4b** and **9b** was performed using the C18 Luna® semi-preparative column with a gradient elution of ACN (10–90% in H_2O, containing 0.01% TFA) using a flow rate of 3 mL/min for 30 min. Quality control of the radiolabeled compounds, as well as the stability studies, were carried out on a Waters Acquity Arc ultra-high performance liquid chromatography (UHPLC) system equipped with a diode array detector and a radio-detector from Canberra (Zelik, Belgium) using a Phenomenex C-18 Gemini® analytical column (250.0 × 4.6 mm, 5 µm) with a gradient elution of ACN (5–95% in H_2O, containing 0.1% TFA) using a flow rate of 1 mL/min for 30 min.

2.2 Chemistry

2.2.1 2,2′,2″-(10-(2-(((*S*)-6-Azido-1-(((*S*)-1,6-diamino-1-oxohexan-2-yl)amino)-1-oxohexan-2-yl)amino)-2-oxoethyl)-1,4,7,10-tetraazacyclododecane-1,4,7-triyl)triacetic acid (2)

Loading of Fmoc-Lys(Boc)-OH (0.5 mmol, 2 equiv.) onto the Rink Amide 4-methylbenzhydrylamine (MBHA) resin (370 mg; average loading capacity, 0.678 mmol/g) was carried out using solutions of 1-[bis(dimethylamino)methylene]-1*H*-1,2,3-triazolo

[4,5-b]pyridinium 3-oxide hexafluorophosphate (HATU; 0.25 M, 2 mL, 2 equiv.) and *N*,*N*-diisopropylethylamine (DIPEA; 0.50 M, 2 mL, 4 equiv.) in DMF. The beads were shaken for 2 h at room temperature (rt). Capping of the beads was achieved using a mixture of acetic anhydride (1.18 mL, 12.5 mmol, 50 equiv.) and 1 M DIPEA (2.19 mL, 12.5 mmol, 50 equiv.) for 30 min at rt. The *N*-terminal Fmoc protecting group was removed by treatment of the resin with a solution containing 20% piperidine in DMF (6 mL) for 13 min at rt. Fmoc-Lys(N_3)-OH (198 mg, 0.5 mmol, 2 equiv.) was coupled following the protocol described earlier. After Fmoc removal, the peptidyl-resin was treated overnight with DOTA-NHS ester (382 mg, 0.5 mmol, 2 equiv.) and triethylamine (Et_3N; 315 µL, 2.2 mmol, 9 equiv.) in DMF (4 mL) to obtain **1**. Cleavage and removal of the Boc protecting group were carried out using a mixture of trifluoroacetic acid/triisopropylsilane/water (TFA/TIS/H_2O; 5 mL, v/v/v = 95:2.5:2.5). The beads were stirred for 2 h and washed twice with the cleavage cocktail. TFA was removed by air stream, and the crude compound **2** was precipitated and washed by the addition of cold diethyl ether and collected by centrifugation. Compound **2** was collected as a crude yellow solid (294 mg, 12.8%). Analytical retention time: t_R = 1.1 min. ESI-MS: *m*/*z*, determined: 685.8 $C_{28}H_{51}N_{11}O_9$, obtained: 686.3 $[M + H]^+$.

2.2.2 2,2′,2″-(10-(2-(((*S*)-1-(((*S*)-1,6-Diamino-1-oxohexan-2-yl)amino)-6-(8-(3-(3-(2,5-dioxo-2,5-dihydro-1*H*-pyrrol-1-yl)propanamido)propanoyl)-8,9-dihydro-1*H*-dibenzo[*b*,*f*][1,2,3]triazolo[4,5-d]azocin-1-yl)-1-oxohexan-2-yl)amino)-2-oxoethyl)-1,4,7,10-tetraazacyclododecane-1,4,7-triyl)triacetic acid (3)

Compound **2** (74 mg, 0.107 mmol) and DBCO-maleimide (50 mg, 0.118 mmol, 1.1 equiv.) in MeOH (2 mL) were stirred for 30 min at 37°C. The solvent was evaporated under vacuum, and the crude residue was dissolved in a mixture of H_2O/ACN (2 mL, v/v = 1:1) for preparative HPLC purification. Compound **3** was collected as a white powder (54 mg, 45%). Analytical retention time: t_R = 3.5 min (Figure S1a). Chemical purity >93%. ESI-MS: *m*/*z*, determined: 1112.5 $C_{53}H_{72}N_{14}O_{13}$, obtained: 557.4 $[M + 2H]^{2+}$ (Figure S1b).

2.2.3 2,2′,2″-(10-(2-(((*S*)-1-(((*S*)-1-Amino-6-(4-(4-iodophenyl)butanamido)-1-oxohexan-2-yl)amino)-6-(8-(3-(3-(2,5-dioxo-2,5-dihydro-1*H*-pyrrol-1-yl)propanamido)propanoyl)-8,9-dihydro-1*H*-dibenzo[*b*,*f*][1,2,3]triazolo[4,5-d]azocin-1-yl)-1-oxohexan-2-yl)amino)-2-oxoethyl)-1,4,7,10-tetraazacyclododecane-1,4,7-triyl)triacetic acid (4a)

2,5-Dioxopyrrolidin-1-yl 4-(4-iodophenyl)butanoate (AB-NHS ester) was synthesized as previously described [5]. Compound **3** (20 mg, 0.018 mmol) was added to a solution of AB-NHS ester (10 mg, 0.027 mmol, 1.5 equiv.) and Et_3N (5 µL, 0.036 mmol, 2 equiv.) in H_2O/ACN (2 mL, v/v = 1:1). The reaction mixture was stirred for 1 h at rt. Then, the product was purified by preparative HPLC to give **4a** as a white solid (12.5 mg, 50%). Analytical retention time: t_R = 4.5 min (Figure S2a). Chemical purity >97%. ESI-MS: *m*/*z*, determined: 1384.5 $C_{63}H_{81}IN_{14}O_{14}$, obtained: 1385.5 $[M + H]^+$ and 693.4 $[M + 2H]^{2+}$ (Figure S3a).

2.2.4 2,2′,2″-(10-(2-(((2)-1-(((2*S*)-1-Amino-6-(((((*E*)-cyclooct-4-en-1-yl)oxy)carbonyl)amino)-1-oxohexan-2-yl)amino)-6-(8-(3-(3-(2,5-dioxo-2,5-dihydro-1*H*-pyrrol-1-yl)propanamido)propanoyl)-8,9-dihydro-1*H*-dibenzo[*b*,*f*][1,2,3]triazolo[4,5-d]azocin-1-yl)-1-oxohexan-2-yl)amino)-2-oxoethyl)-1,4,7,10-tetraazacyclododecane-1,4,7-triyl)triacetic acid (4b)

Treatment of **3** (20 mg, 0.018 mmol) with (*E*)-cyclooct-4-enyl-2,5-dioxo-1-pyrrolidinyl carbonate (TCO-NHS ester; 7.2 mg, 0.027 mmol, 1.5 equiv.) and Et_3N (2.5 µL, 0.018 mmol, 1 equiv.) in H_2O/ACN (2 mL, v/v = 1:1) during 1 h at rt provided **4b** after semi-preparative HPLC purification. Compound **4b** was collected as a white solid (6.5 mg, 29%). Analytical retention time: t_R = 4.4 min (Figure S2b). Chemical purity >98%. ESI-MS: *m*/*z*, determined: 1264.6 $C_{62}H_{84}N_{14}O_{15}$, obtained: 1265.6 $[M + H]^+$ (Figure S3b).

2.2.5 SH-CH_2-C(O)-Cpa-c[D-Cys-Aph(Hor)-D-Aph(Cbm)-Lys-Thr-Cys]-D-Tyr-NH_2 (8)

Fmoc-Phe(4-Cl)-D-Cys(Acm)-Aph(Hor)-D-Aph(*t*Bu-Cbm-Lys(Boc)-Thr(*t*Bu)-Cys(Acm)-D-Tyr(*t*Bu) coupled to the resin (**5**) was obtained by sequential coupling of each amino acid for 1 h at rt in the presence of a solution of HATU (0.25 M, 2 mL, 0.5 mmol, 2 equiv.) and DIPEA (0.5 M, 2 mL, 1 mmol, 4 equiv.) in DMF. Fmoc deprotection was accomplished by treatment of the resin with a 20% solution of piperidine in DMF (6 mL) for 13 min at rt. Amide formation and Fmoc deprotection were monitored by Kaiser and TNBS tests. Coupling and deprotection were repeated when the reaction was not complete. Fmoc-D-Tyr(*t*Bu)-OH (231 mg, 0.5 mmol, 2 equiv.) was loaded onto the Rink Amide MBHA resin (370 mg, average loading capacity: 0.678 mmol/g). The beads were shaken for 2 h at rt. Capping of the resin was carried out using a mixture of acetic anhydride (1.18 mL, 12.5 mmol, 50 equiv.) and DIPEA (1 M, 2.19 mL, 12.5 mmol, 50 equiv.) for 1 h at rt. Fmoc removal and coupling with Fmoc-Cys(Acm)-OH (208 mg, 0.5 mmol, 2 equiv.), Fmoc-L-Thr(*t*Bu)-OH (199 mg,

0.5 mmol, 2 equiv.), Fmoc-L-Lys(Boc)-OH (235 mg, 0.5 mmol, 2 equiv.), Fmoc-D-Aph(*t*Bu-Cbm)-OH (252 mg, 0.5 mmol, 2 equiv.), Fmoc-Aph(Hor)-OH (272 mg, 0.5 mmol, 2 equiv.), Fmoc-D-Cys (Acm)-OH (208 mg, 0.5 mmol, 2 equiv.) and Fmoc-Phe(4-Cl)-OH (212 mg, 0.5 mmol, 2 equiv.) were achieved following the protocol described earlier. Cyclization of the peptide was accomplished using thallium(III) trifluoroacetate (273 mg, 0.5 mmol, 2 equiv.) in DMF (4 mL) for 1 h at rt to give **6**. After Fmoc deprotection, the resin was dried and divided into two fractions. The first fraction (~330 mg, 0.12 mmol) was coupled to 2,5-dioxopyrrolidin-1-yl-2-(tritylthio)acetate (108 mg, 0.25 mmol, 2 equiv.), prepared as previously reported [12] The reaction was performed in presence of DIPEA (500 µL, 0.25 mmol, 2 equiv.) and DMF (4 mL) for 3 h at rt. Cleavage and removal of the side-chain protecting groups were achieved using a solution of TFA/TIS/H_2O (2 mL, v/v/v = 95:2.5:2.5) for 2 h at rt to give **8**. The resin was treated twice with the cleavage cocktail, and all liquid phases were pooled. TFA was removed by air stream, and the peptide was precipitated using ice-cold diethyl ether and collected by centrifugation. A second treatment of the crude product with TFA/DCM (2 mL, v/v = 1:1) and triethylsilane (51 µL, 0.32 mmol, 2.5 equiv.) for 30 h at rt was carried out to complete the removal of the *t*Bu protecting groups. The solvents were evaporated under reduced pressure. The compound was treated with ice-cold diethyl ether for precipitation and collected by centrifugation. The residue was dissolved in H_2O/ACN (3 mL, v/v = 1:1) and purified by semi-preparative HPLC. Pure compound **8** was obtained as a white solid (32.6 mg, 9.5%). Analytical retention time: t_R = 3.9 min (Figure S4a). Chemical purity >95%. ESI-MS: *m*/*z*, determined: 1375.4 $C_{60}H_{74}ClN_{15}O_{15}S_3$, obtained: 1376.4 $[M + H]^+$ (Figure S4b).

2.2.6 2,2′,2″-(10-(2-(((2*S*)-6-(8-(3-(3-(3-((2-(((2*S*)-1-(((4 R,7*S*,10*S*,13*S*,16*S*,19 R)-4-(((*S*)-1-Amino-3-(4-hydroxyphenyl)-1-oxopropan-2-yl)carbamoyl)-10-(4-aminobutyl)-16-(4-(2,6-dioxohexahydropyrimidine-4-carboxamido)benzyl)-7-((*S*)-1-hydroxyethyl)-6,9,12,15,18-pentaoxo-13-(4-ureidobenzyl)-1,2-dithia-5,8,11,14,17-pentaazacycloicosan-19-yl)amino)-3-(4-chlorophenyl)-1-oxopropan-2-yl)amino)-2-oxoethyl) thio)-2,5-dioxopyrrolidin-1-yl)propanamido) propanoyl)-8,9-dihydro-1H-dibenzo[*b*,*f*][1,2,3]triazolo [4,5-d]azocin-1-yl)-1-(((*S*)-1-amino-6-(4-(4-iodophenyl) butanamido)-1-oxohexan-2-yl)amino)-1-oxohexan-2-yl)amino)-2-oxoethyl)-1,4,7,10-tetraazacyclododecane-1,4,7-triyl)triacetic acid (9a)

To a solution of **4a** (12.5 mg, 0.009 mmol) in H_2O/ACN (2 mL, v/v = 1:1), **8** (13,7 mg, 0.010 mmol, 1.1 equiv.) was added. The mixture was incubated at 37°C, and the reaction was monitored by LC/MS. Once the reaction was completed (~30 min), the mixture was purified using preparative HPLC to give compound **9a** as a white solid (18.8 mg, 76%). Analytical retention time: t_R = 4.3 min (Figure S5a). Chemical purity >96%. ESI-MS: *m*/*z*, determined: 2759.9 $C_{123}H_{155}ClN_{29}O_{29}S_3$, obtained: 1381.7 $[M + 2H]^{2+}$ (Figure S6a).

2.2.7 2,2′,2″-(10-(2-(((2*S*)-6-(8-(3-(3-(3-((2-(((2*S*)-1-(((4 R,7*S*,10*S*,13*S*,16 *S*,19 R)-4-(((*S*)-1-Amino-3-(4-hydroxyphenyl)-1-oxopropan-2-yl)carbamoyl)-10-(4-aminobutyl)-16-(4-(2,6-dioxohexahydropyrimidine-4-carboxamido)benzyl)-7-((*S*)-1-hydroxyethyl)-6,9,12,15,18-pentaoxo-13-(4-ureidobenzyl)-1,2-dithia-5,8,11,14,17-pentaazacycloicosan-19-yl)amino)-3-(4-chlorophenyl)-1-oxopropan-2-yl)amino)-2-oxoethyl) thio)-2,5-dioxopyrrolidin-1-yl)propanamido) propanoyl)-8,9-dihydro-1*H*-dibenzo[*b*,*f*][1,2,3]triazolo [4,5-d]azocin-1-yl)-1-(((2*S*)-1-amino-6-(((((*E*)-cyclooct-4-en-1-yl)oxy)carbonyl)amino)-1-oxohexan-2-yl)amino)-1-oxohexan-2-yl)amino)-2-oxoethyl)-1,4,7,10-tetraazacyclododecane-1,4,7-triyl)triacetic acid (9b)

Compound **4b** (6.5 mg, 0.005 mmol) reacted with **8** (8.5 mg, 0.006 mmol, 1.2 equiv.) in H_2O/ACN (2 mL, v/v = 1:1). The reaction mixture was incubated at 37°C and was monitored by LC/MS. Once the reaction was completed (~2 h), the crude compound was purified using semi-preparative HPLC to give compound **9b** as a white solid (4.8 mg, 35%). Analytical retention time: t_R = 4.2 min (Figure S5b). Chemical purity >95%. ESI-MS: *m*/*z*, determined: 2642.4 $C_{122}H_{158}ClN_{29}O_{30}S_3$, obtained: 1322.2 $[M + 2H]^{2+}$ (Figure S6b).

2.3 Radiochemistry

2.3.1 Radiolabeling of compounds 9a and 9b with [^{111}In]$InCl_3$

Compound **9a** or **9b** (1 nmol) was added to a mixture of [^{111}In]$InCl_3$ (50 MBq), ascorbic acid/gentisic acid (10 µL, 50 mM), sodium acetate (2.5 M, 1 µL, pH 8), and water containing kolliphor (2.0 mg/mL, 58.6 µL). The labeling mixture (pH 4.5) was incubated at 90°C for 20 min. Then, it was cooled down for 5 min, and the radiochemical yield (RCY) was determined by iTLC on silica gel-impregnated glass-fiber sheets. Diethylenetriaminepentaacetic acid (4 mM, 5 µL) was added to complex-free indium-111. The radiochemical purity (RCP) of the ^{111}In-labeled peptides was measured by radio-HPLC (Figure S7a and b).

2.3.2 Determination of the distribution coefficient ($LogD_{7.4}$) of [^{111}In]In-9a and [^{111}In]In-9b

The distribution coefficient of [^{111}In]In-**9a** and [^{111}In]In-**9b** was determined by the shake-flask method. The experiment was performed in triplicate for each compound. The radiopeptides (~0.3 MBq) were added to a mixture of phosphate-buffered saline (PBS)/*n*-octanol (1 mL, v/v = 1:1) in Eppendorf vials. The Eppendorf vials were vortexed vigorously and centrifuged for 3 min at 10,000 rpm. *n*-Octanol was separated from PBS and poured into new vials. Samples from each phase (10 µL) were poured into glass tubes and measured with a gamma counter. The $LogD_{7.4}$ value was calculated using the following equation: $LogD_{7.4} = \log_{10}$ ([counts in organic phase]/[counts in aqueous phase]).

2.3.3 Stability studies in PBS buffer and mouse serum

The ^{111}In-labeled peptides (~0.3 MBq) were incubated in either PBS (250 µL) or mouse serum (125 µL) (Merck, Haarlerbergweg, The Netherlands) at 37°C. The inertness of the radiopeptides was checked at 1 and 3 h post incubation. Precipitation of the proteins in mouse serum was achieved by the addition of an equal volume of ACN to the mixture. The vial was vortexed and centrifuged at 10,000 rpm for 20 min. Stability studies in both media were monitored by radio-HPLC (Figures S8 and S9).

3 Results and discussion

Our synthetic approach aimed at the design of a building block allowing the incorporation of two different functional groups into the chemical structure of peptide-based biovector. The building block featured three different attachment points. A DOTA chelator was first introduced during SPPS since the chelator is not sensitive to the harsh reaction conditions experienced during the synthesis, such as the strong acidic conditions employed during the cleavage of the peptide from the resin. The DOTA chelator was chosen due to its clinical relevance and its capability to complex a broad variety of radioisotopes. However, other chelators (e.g., NOTA, DFO) could have been coupled to the building block [13]. Then, an azidolysine and a natural lysine residue were introduced into the building block to offer two additional attachment points. The presence of the two different attachment points warranted the orthogonal attachment of the building block to the biovector and the incorporation of the second functional group. The SPAAC click reaction was employed with the azidolysine due to its selectivity, favorable PK, and orthogonality allowing the obtention of the desired compounds under friendly conditions [14]. The second functional group was introduced on the building block via an amide formation with the remaining lysine. Our synthetic route confirmed that the desired products could be obtained in the liquid phase and allowed the incorporation of sensitive functional groups at the last step of the synthesis.

Several investigations have demonstrated that the incorporation of two different functional groups can be performed by coupling onto lysine residues directly inserted into the amino acid sequence of a peptide [5,6,15]. However, the success of this approach is mainly depending on the presence of other lysine residues in the original peptide sequence. Moreover, regioselectivity of the introduction of the functional groups on the biovector is sparsely achieved, unless different protecting groups for the side-chain amino groups of the lysine residues are considered during the synthesis. However, this approach significantly complicates the synthetic pathway, and the deprotection conditions are not always compatible with the inserted functional groups (i.e., removal of an ivDde-protecting group with hydrazine and groups containing a carbonyl function). Our chemical approach overcomes these limitations by allowing the orthogonal incorporation of the functional groups via straightforward chemical reactions, known to occur in smooth reaction conditions and with high chemical yields. Furthermore, the regioselective attachment of the building block on the biovector enables to selection of a position at which the chemical modification has less influence on the biochemical properties of the parent peptide.

The orthogonality of the building block was confirmed by performing a SPAAC click reaction with a DBCO-maleimide linker prior to its conjugation to the biovector. We decided to add a linker to avoid the steric hindrance that could be caused by the bulky building block. The linker provides more space between the building block and the peptide, allowing better coupling efficiency and less effect on the binding properties of the peptide. However, the addition of the linker would likely not be required with larger biovectors, such as antibodies and proteins. Furthermore, the derivatization of the building block with a maleimide group enhances its utility, as it enables the conjugation of the building block to antibodies or antibody fragments. Indeed, those large biomolecules are usually functionalized with a chelator, a fluorescent dye, or a drug on a cysteine via the thiol–maleimide Michael addition. Therefore, the maleimide version of our building block could facilitate the dual functionalization of these large and sensitive biovectors [16].

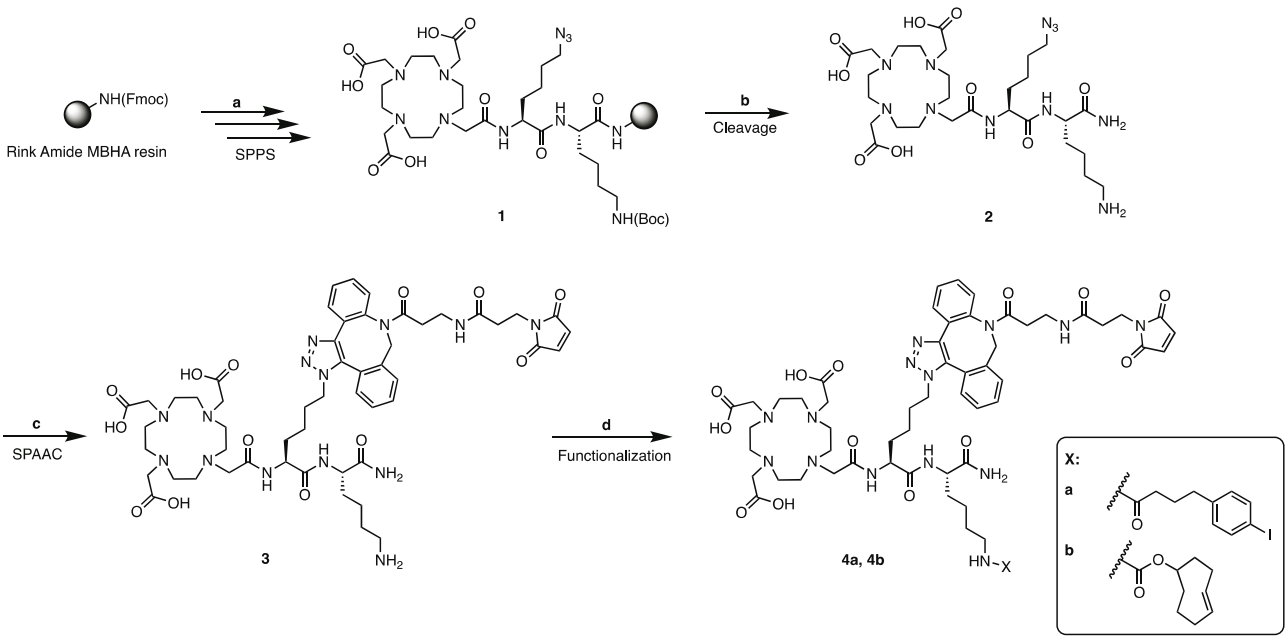

Scheme 1: Synthesis of the dual-functionalized building blocks (**4a** and **4b**). Reagents and conditions: (a) Fmoc-SPPS; (b) TFA/TIS/H_2O, 2 h, rt, 22%; (c) DBCO-maleimide, MeOH, 30 min, 37°C, 45%; (d) AB-NHS ester or TCO-NHS ester, Et_3N, H_2O/ACN, 1 h, rt, 50% and 29%, respectively.

Compound **3** was a key intermediate in our synthetic approach due to its ability to be derivatized with a broad variety of functional groups, such as fluorescent dyes (IRDye800CW, Cy5 derivatives), pharmacokinetic modifiers, and cytotoxic drugs. A large library of compounds could therefore be obtained by the conjugation of various chemical entities to the free lysine. As a proof-of-concept, we decided to functionalize **3** with either an albumin-binding moiety or a click handle. The 4-(*p*-iodophenyl)butanoic acid was selected as it has been widely applied to extend the blood circulation of radioligands (e.g., prostate specific membrane antigen, folic acid, and DOTA-TATE) by binding to albumin with a good affinity [17–20]. The TCO group was chosen due to its high sensitivity towards acidic conditions, requiring flexibility in the synthesis of the building block and its incorporation into **3** at the last step of the synthesis [21]. TCO was incorporated into the building block to facilitate pretargeting applications [22]. Compounds **4a** and **4b** were obtained by the SPAAC click reaction between the azido intermediate **2** and the DBCO-maleimide linker, followed by the conjugation of the activated succinimidyl AB-NHS and TCO-NHS esters (Scheme 1). This route provided **4a** and **4b** with 50 and 29% yield, respectively, after HPLC purification. The purity of **4a** and **4b** was determined by analytical HPLC and was found to be higher than 97 and 98%, respectively.

As mentioned earlier, the thiol group of the cysteine residues is commonly used to conjugate diverse functional groups to antibodies. Therefore, to mimic this situation, we attached a short thiolated linker at the *N*-terminal position of our model cyclic peptide JR11. We chose to demonstrate the application of our building block on a peptide since, like antibodies, peptides are constituted of amino acids but their chemistry is less challenging. Compound **8** was obtained by Fmoc-based SPPS on a Rink Amide MBHA resin, followed by cyclization of the peptide on resin by treatment with $Tl(TFA)_3$, Fmoc deprotection, conjugation of the succinimidyl ester of (tritylthio)acetic acid at the *N*-terminus, cleavage, and deprotection of the side-chain protective groups [12]. Compound **8** was obtained in 9.5% yield after HPLC purification with a purity higher than 95% (determined by analytical HPLC; Scheme 2).

The final dual-functionalized compounds **9a** and **9b** were prepared by the conjugation of either **4a** or **4b** with **8** (Scheme 2). The thiol–maleimide Michael reaction was performed in a mixture of H_2O/ACN, and the conversion of compound **8** into the desired compounds **9a** and **9b** was observed in only 30 min at 37°C. During the reaction, we added a co-solvent, namely ACN, to improve the solubility of the peptides and the building block, but this reaction can typically be performed under biologically friendly conditions. Compounds **9a** and **9b** were obtained 76 and 35% yield, respectively, after HPLC purification. The difference in chemical yields might be explained by the difference in the purification methods and the need to use less acidic solvent to purify **9b** in order to avoid its isomerization into the *cis*-isomer. It has been shown that *cis*-cyclooctene (CCO)

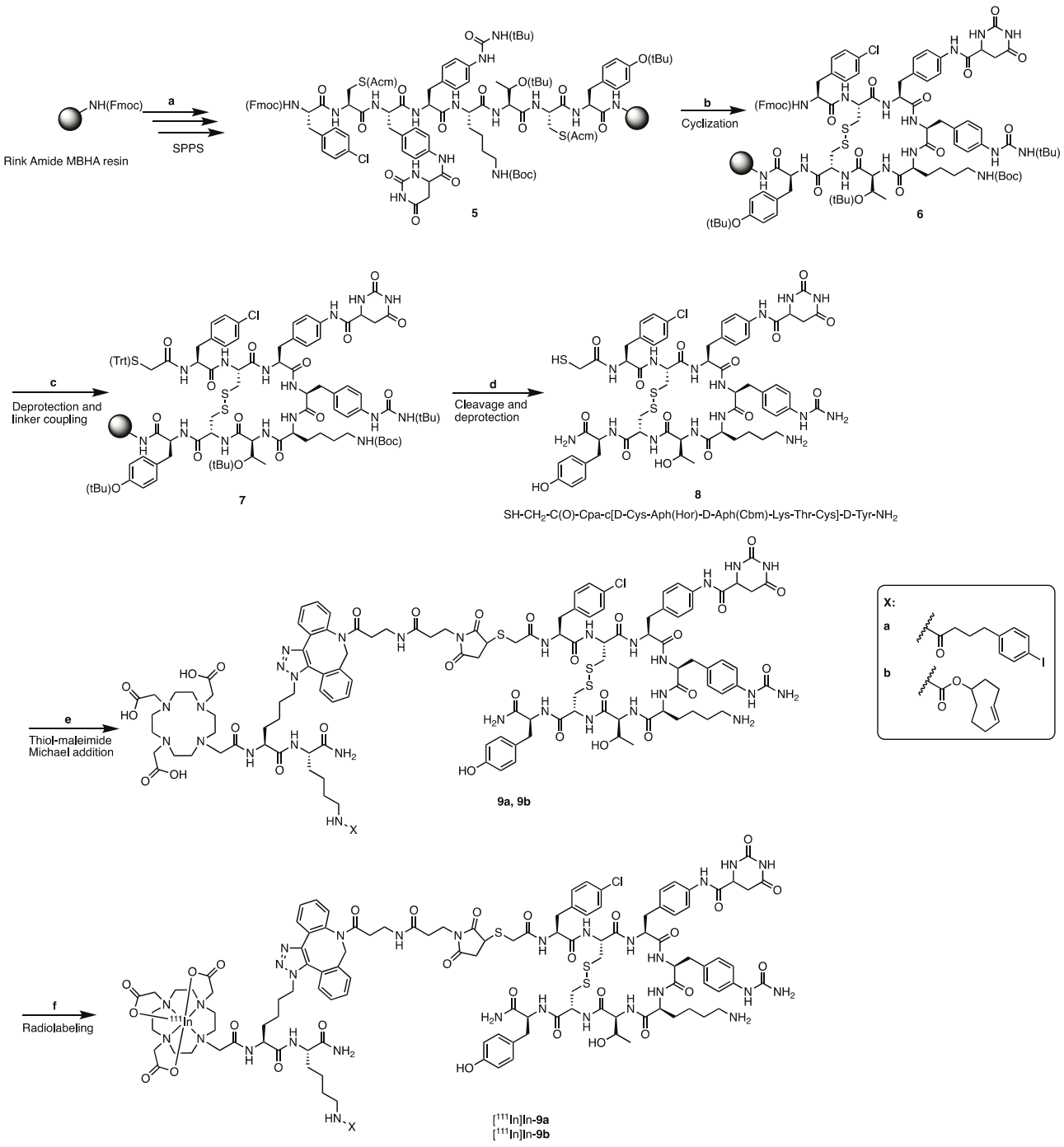

Scheme 2: Synthesis of compound **8**. Reagents and conditions: (a) Fmoc-SPPS; (b) $Tl(TFA)_3$, DMF, 1 h, rt; (c) (i) 20% piperidine in DMF, 13 min, rt, (ii) TrtS-CH_2-OSu, DIPEA, DMF, 3 h, rt; (d) (i) TFA/TIS/H_2O, 2 h, rt and (ii) TFA/DCM, 30 h, rt, 9.5%; (e) **4a** or **4b**, H_2O/ACN, 37°C, 76% and 35%, respectively. (f) [^{111}In]$InCl_3$, **9a** or **9b**, gentisic/ascorbic acid, sodium acetate, 20 min, 90°C, 96.3, and 96.1% respectively.

is less reactive than TCO toward tetrazines during the IEDDA reaction [21]. **9a** and **9b** were characterized by MS, and their purity, determined by analytical HPLC, was higher than 96 and 95%, respectively.

Subsequently, **9a** and **9b** were radiolabeled with [^{111}In] $InCl_3$ using gentisic and ascorbic acid. Both substances are quenchers, known to protect the radiolabeled peptides against radiolysis [23]. It has been reported that ascorbic acid reacts with the main radicals formed by gentisic acid and reduces them into the original gentisic acid found in the initial dosage form [24]. Kolliphor, a well-known solubilizer and emulsifier, was added to the radiolabeling

Table 1: RCYs (n = 2), RCPs (n = 2), stability studies in PBS (n = 1), and mouse serum (n = 1) and determination of the partition coefficient ($LogD_{7.4}$) (n = 3) of [^{111}In]In-**9a** and [^{111}In]In-**9b**

	RCY (%)	RCP (%)	Stability in PBS (%)*		Stability in mouse serum (%)*		$LogD_{7.4}$
			1 h	3 h	1 h	3 h	
[^{111}In]In-**9a**	96.3 ± 0.7	94.9 ± 1.5	90.4	90.9	94.1	94.9	−0.59 ± 0.05
[^{111}In]In-**9b**	96.1 ± 2.3	86.0 ± 3.3	76.3	75.1	93.7	92.5	−0.66 ± 0.02

*Results are presented as a percentage of intact radiopeptide after incubation at 37°C.

mixture in order to improve the solubility of the radiolabeled peptides and reduce their stickiness. Radiolabeling of both compounds with [^{111}In]$InCl_3$, using a molar activity of 50 MBq/nmol, was successful and comparable to what has been recently published with other DOTA-JR11 analogs [5]. It confirms that the chemical modifications did not hamper the efficiency of the complexation of $^{111}In^{3+}$ by the DOTA chelator. The RCY and RCP of both radiopeptides are presented in Table 1. [^{111}In]In-**9a** and [^{111}In]In-**9b** were obtained in 96.3 and 96.1% RCY and 94.9 and 86.0% RCP, respectively. Next, we determined the stability of both radiopeptides in PBS (pH 7.4) and mouse serum at 1 and 3 h after incubation at 37°C. [^{111}In]In-**9a** and [^{111}In]In-**9b** exhibited good stability in mouse serum (>92% intact radiopeptides at 3 h), demonstrating their inertness toward peptidase digestion. However, [^{111}In]In-**9a** showed a better stability in PBS compared to [^{111}In]In-**9b** (90.9% intact [^{111}In]In-**9a** vs 75.1% intact [^{111}In]In-**9b** at 3 h). It might be explained by the presence of the carbamate bond between the TCO and the side chain of the lysine residue. Indeed, it has been previously reported that the carbamate linkage is sensitive to radiolysis [25].

The distribution coefficient was determined by the shake-flask method. Both radiopeptides displayed a $LogD_{7.4}$ value higher than the parent peptide DOTA-JR11 (−0.59 and −0.66 for [^{111}In]In-**9a** and [^{111}In]In-**9b** vs −2.5 for [^{177}Lu]Lu-DOTA-JR11) [26]. The introduction of lipophilic chemical groups, such as DBCO, AB, and TCO in the chemical structure of the DOTA-JR11 logically affected the hydrophilicity of the final molecules.

In the previous examples, a chelator, an albumin-binding moiety, and a click handle were introduced into the dual-functionalized building block. However, the presence of the azide and amine groups on the molecule confers full orthogonality to attach selectively various chemical entities. We showed that the insertion of a maleimide into our building block offers the opportunity to functionalize other biovectors, such as antibodies, in a single step through the thiol–maleimide Michael reaction. The reaction proceeded quickly in biologically friendly conditions (aqueous medium and physiological temperature), allowing the radiolabeling of the building block in harsh reaction conditions (i.e., heating in acidic solution) before its conjugation to a fragile biomolecule [27].

4 Conclusion

In our study, we presented a versatile approach allowing the orthogonal incorporation of different functional groups (DOTA chelator, AB, and TCO) into a building block that can be attached to biovectors in a single step via a SPAAC or thiol–maleimide Michael reaction. Our proof-of-concept was demonstrated by the preparation of two different dual-functionalized building blocks, **4a** and **4b**, which were coupled to the free sulfhydryl group of a cyclic peptide. Both final compounds, **9a** and **9b**, were obtained in very high chemical purities, and successfully radiolabeled with [^{111}In]$InCl_3$. We confirmed that the chemical remodeling of the peptides did not hamper the complexation of the radionuclide by the chelator, and high stability of the final radiopeptides was demonstrated in PBS and mouse serum. Consequently, this synthetic approach could be very valuable for the functionalization of radiolabeled biovectors.

Acknowledgments: We are grateful to the Dutch Cancer Society (KWF) for the financial support and the Department of Radiology and Nuclear Medicine at the Erasmus MC for technical assistance.

Funding information: This research was funded by the Dutch Cancer Society (KWF), grant number 12259.

Author contributions: Conceptualization, Y.S.; methodology, M.H. and Y.S.; software, M.H.; validation, M.H.; formal analysis, M.H. and D.C.; investigation, M.H., D.C., and Y.S.; resources, Y.S.; data curation, M.H. and D.C.; writing – original draft preparation, M.H.; writing – review and editing, M.H., D.C., and Y.S.; visualization, Y.S.; supervision, Y.S.; project administration, Y.S.; funding acquisition, Y.S. All authors have read and agreed to the published version of the manuscript.

Conflict of interest: The authors do not declare any conflicts of interest.

Ethical approval: The conducted research is not related to either human or animal use.

Data availability statement: All data generated or analyzed during this study are included in this published article and its supplementary information file.

References

[1] Dalm SU, Bakker IL, De Blois E, Doeswijk GN, Konijnenberg MW, Orlandi F, et al. 68Ga/177Lu-NeoBOMB1, a novel radiolabeled GRPR antagonist for theranostic use in oncology. J Nucl Med. 2017;58:293–9.

[2] Sanli Y, Garg I, Kandathil A, Kendi T, Baladron Zanetti MJ, Kuyumcu S, et al. Neuroendocrine tumor diagnosis and management: 68 Ga-DOTATATE PET/CT. AJR. 2018;211:267–77.

[3] Kuil J, Velders AH, Van Leeuwen FWB. Multimodal tumor-targeting peptides functionalized with both a radio- and a fluorescent label. Bioconjug Chem. 2010;21:1709–19.

[4] Bumbaca B, Li Z, Shah DK. Pharmacokinetics of protein and peptide conjugates. Drug Metab Pharmacokinet. 2019;34:42–54.

[5] Koustoulidou S, Handula M, de Ridder C, Stuurman D, Beekman S, de Jong M, et al. Synthesis and evaluation of two long-acting sstr2 antagonists for radionuclide therapy of neuroendocrine tumors. Pharmaceuticals . 2022;15:1–15.

[6] Handula M, Verhoeven M, Chen K, Haeck, Jong J, De M, et al. Towards complete tumor resection: novel dual-modality probes for improved image-guided surgery of grpr-expressing prostate cancer. Pharmaceutics. 2022;14:1–18.

[7] Strekowski L, Mason CC, Lee H, Patonay G. Synthesis of a functionalized cyanine dye for covalent labeling of biomolecules with a pH-sensitive chromophore. Heterocycl Comm. 2004;10:381–2.

[8] Rossin R, Van Den Bosch SM, Ten Hoeve W, Carvelli M, Versteegen RM, Lub J, et al. Highly reactive trans-cyclooctene tags with improved stability for diels-alder chemistry in living systems. Bioconjug Chem. 2013;24:1210–7.

[9] Chen KT, Nieuwenhuizen J, Handula M, Seimbille Y. A novel clickable MSAP agent for dual fluorescence/nuclear labeling of biovectors. Org Biomol Chem. 2020;18:6134–9.

[10] Garanger E, Aikawa E, Reynolds F, Weissleder R, Josephson L. Simplified syntheses of complex multifunctional nanomaterials. ChemComm . 2008;39:4792–4.

[11] Handula M, Chen KT, Seimbille Y. Iedda: An attractive bioorthogonal reaction for biomedical applications. Molecules. 2021;26:1–20.

[12] Chen X, Li L, Liu F, Liu B. Synthesis and biological evaluation of technetium-99m-labeled deoxyglucose derivatives as imaging agents for tumor. Bioorganic Med Chem Lett. 2006;16:5503–6.

[13] Stasiuk GJ, Long NJ. The ubiquitous DOTA and its derivatives: The impact of 1,4,7,10-tetraazacyclododecane-1,4,7,10-tetraacetic acid on biomedical imaging. ChemComm. 2013;49:2732–46.

[14] Deng Y, Shavandi A, Okoro OV, Nie L. Alginate modification via click chemistry for biomedical applications. Carbohydr Polym. 2021;270:1–18.

[15] Zhang H, Desai P, Koike Y, Houghton J, Carlin S, Tandon N, et al. Dual-modality imaging of prostate cancer with a fluorescent and radiogallium-labeled gastrin-releasing peptide receptor antagonist. J Nucl Med. 2017;58:29–35.

[16] Nair DP, Podgórski M, Chatani S, Gong T, Xi W, Fenoli CR, et al. The Thiol-Michael addition click reaction: A powerful and widely used tool in materials chemistry. Chem Mater. 2014;26:724–44.

[17] Müller C, Struthers H, Winiger C, Zhernosekov K, Schibli R. DOTA conjugate with an albumin-binding entity enables the first folic acid-targeted 177Lu-radionuclide tumor therapy in mice. J Nucl Med. 2013;54:124–31.

[18] Tiel S, vanTiel van S, Maina T, Nock B, Konijnenberg M, Blois E, de, et al. Albutate-1, a novel long-circulating radiotracer targeting the somatostatin receptor subtype 2. J Nucl Med Radiat Sci. 2021;2:1–9.

[19] Rousseau E, Lau J, Zhang Z, Uribe CF, Kuo HT, Zhang C, et al. Effects of adding an albumin binder chain on [177Lu]Lu-DOTATATE. Nucl Med Biol. 2018;66:10–7.

[20] Kuo HT, Lin KS, Zhang Z, Uribe CF, Merkens H, Zhang C, et al. 177Lu-labeled albumin-binder-conjugated PSMA-targeting agents with extremely high tumor uptake and enhanced tumor-to-kidney absorbed dose ratio. J Nucl Med. 2021;62:521–7.

[21] La–Venia A, Dzijak R, Rampmaier R, Vrabel M. An optimized protocol for the synthesis of peptides containing trans-cyclooctene and bicyclononyne dienophiles as useful multifunctional bioorthogonal probes. Chem Eur J. 2021;27:13632–41.

[22] Keinänen O, Fung K, Pourat J, Jallinoja V, Vivier D, Pillarsetty NVK, et al. Pretargeting of internalizing trastuzumab and cetuximab with a 18F-tetrazine tracer in xenograft models. EJNMMI Res. 2017;7:1–12.

[23] de Blois E, Sze Chan H, Konijnenberg M, de Zanger R, Breeman AP, W. Effectiveness of quenchers to reduce radiolysis of 111In- or 177Lu-labelled methionine-containing regulatory peptidesMaintaining radiochemical purity as measured by HPLC. Curr Top Med Chem. 2013;12:2677–85.

[24] Larenkov A, Mitrofanov I, Pavlenko E, Rakhimov M. Radiolysis-associated decrease in radiochemical purity of 177Lu-radiopharmaceuticals and comparison of the effectiveness of selected quenchers against this process. Molecules. 2023;28:1–26.

[25] Wang WF, Schuchmann MM, Schuchmann HP, Knolle W, Von Sonntag J, Von Sonntag C. Radical cations in the OH-radical-induced oxidation of thiourea and tetramethylthiourea in aqueous solution. J Am Chem Soc. 1999;121:238–45.

[26] Rylova SN, Stoykow C, Del Pozzo L, Abiraj K, Tamma ML, Kiefer Y, et al. The somatostatin receptor 2 antagonist 64Cu-NODAGA-JR11 outperforms 64Cu-DOTA-TATE in a mouse xenograft model. PLoS One. 2018;13:1–6.

[27] Daniel RM, Cowan DA. Biomolecular stability and life at high temperatures. Cell Mol Life Sci. 2000;57:250−64.